J Mater Sci (2007) 42:8334–8341
DOI 10.1007/s10853-006-0252-z

Determination of crystallographic orientation of dwell-fatigue fracture facets in Ti-6242 alloy

V. Sinha · M. J. Mills · J. C. Williams

Received: 4 February 2005 / Accepted: 5 October 2005 / Published online: 1 May 2007

Abstract A technique to determine the crystallographic orientation of the fracture facets has been described. The spatial orientation of the facet plane is determined in a scanning electron microscope (SEM) using a quantitative tilt fractography technique. The crystallographic orientation of the grain, across which a particular fracture facet had been produced, is determined using the electron backscattered diffraction (EBSD) technique in an SEM. These two pieces of information were combined to obtain the crystallographic orientation of the fracture facet normal. This technique was used for the characterization of dwell-fatigue fracture facets at the crack-initiation site in Ti-6242 alloy. Our results indicate that these facets are not exactly aligned with the basal plane, but are inclined at ~10° to it.

Introduction

Faceted initiation site has been observed on the fracture surface of various near - α titanium alloys that were tested under different loading conditions [1–5]. Davidson and Eylon [1] have determined the crystallographic orientation of facets in Ti-alloys using the electron channeling technique in an SEM. In this technique, the SEM stage rotate and tilt controls were adjusted to bring the plane of the facet perpendicular to the electron optic axis. Furthermore, obtaining electron channeling patterns directly from the fracture facets was difficult and the facets were electropolished before being characterized using this technique [1].

The advances in the EBSD technique over the past decade have made it possible to obtain the EBSD patterns directly from the fracture facet. Bache et al. [3] were able to obtain EBSD patterns from fracture facets in a Ti-alloy after lightly etching them. However, it is not clear from their work [3] if and how they accounted for the spatial orientation (i.e. the orientation in space) of the facets. Themelis et al. [6] have described a quantitative tilt fractography technique for the determination of the spatial orientation of the facet plane. This technique, in essence, involves the analyses of the fractographs obtained using an SEM at two different tilt angles.

In several studies on other alloys, the importance of determination of spatial orientation of fracture facets for a complete and accurate characterization of crystallography of facets has been discussed [7–9]. Semprimoschnig et al. [7] have described a methodology to determine the crystallography of cleavage planes, which essentially consists of EBSD characterization of facets and an SEM-based stereo-photogrammetric analysis for automatic fracture surface reconstruction that provides the three-dimensional digital elevation model of the selected area of the fracture surface. They have used this methodology to determine the crystallography of cleavage planes in Armco iron [7]. Davies et al. [8] have used a similar methodology to determine the crystallographic orientation of cleavage facets in steel. Furthermore, Slavik et al. [9] have used EBSD analysis on a metallographic section through the

V. Sinha (✉)
Materials and Processes Division, UES, Inc.,
4401 Dayton-Xenia Road, Dayton, OH 45432, USA
e-mail: vikas.sinha@wpafb.af.mil

M. J. Mills · J. C. Williams
Department of Materials Science and Engineering,
The Ohio State University, 477 Watts Hall, 2041 College Road,
Columbus, OH 43210, USA

fracture surface coupled with a quantitative tilt fractography technique on the facets to determine the crystallography of the fracture facets in an Al-alloy.

In the present work, a similar technique for the determination of crystallographic orientation of fracture facets at the crack-initiation site in Ti-6242 alloy has been described. The spatial orientation of the facet plane was determined using a modified version of the technique of Themelis et al. [6]. The EBSD patterns were obtained directly from the fracture facets in an SEM and they were indexed in order to determine the crystallographic orientation of the grains across which the facets had been produced. The crystallographic orientations of the fracture facets are presented as inverse pole figures in which both pieces of information (crystallographic orientation of the grain determined by EBSD analysis and spatial orientation of the facet plane determined by quantitative tilt fractography), obtained in an SEM, are combined.

In another study [10], the technique presented in the current work has been used to characterize the fracture facets in Ti-6242 alloy that are produced under different loading conditions.

Experimental procedures

Material and specimen

The Ti-6Al-2Sn-4Zr-2Mo (+Si) alloy that was used in this study was provided in the form of a pancake forging by Ladish Co., Cudahy, WI. The as-received alloy had a bimodal microstructure, consisting of primary α grains and transformed β regions (Fig. 1). A more detailed description of microstructure, macro-texture and micro-texture of the as-received alloy is presented elsewhere [5]. This material had a high level of micro-texture that has been shown to correspond to a large dwell life debit in this alloy system [4].

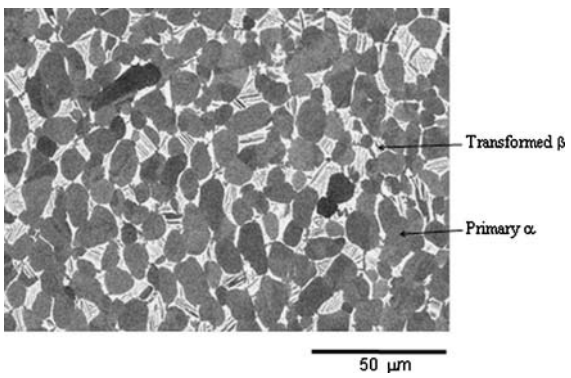

Fig. 1 SEM micrograph of the as-received α/β forged Ti-6242 alloy, acquired using a backscattered electron detector

The dwell-fatigue specimen examined in this investigation is taken from a previously reported work [5]. The peak stress during dwell-fatigue testing of this specimen was ~95% of yield strength (see Ref. [5] for details). As has been described in Ref. [5], the initiation site consisted of faceted features for this test condition. The fractured dwell-fatigue specimen was cleaned in an ultrasonic cleaner with acetone and then, with methanol. Thereafter, the specimen was baked overnight in an oven kept at ~70 °C before being characterized in an SEM.

SEM examination

The SEM used in the current study is a Philips XL-30 ESEM instrument that has a field emission gun (FEG) as the electron source. The crystallographic orientation of the grains, across which the dwell-fatigue fracture facets had been produced, was determined using the EBSD technique in the SEM. The details of the EBSD technique have been described elsewhere [11]. A critical step in applying this technique for the analysis of the fracture facets is the collection of background signal, which is typically collected at a low magnification on the sample being characterized for the case of polished specimens. Due to the unevenness of the fracture surface, a good background signal was difficult to obtain directly from the faceted fracture region. Therefore, the background signal was collected from a polished polycrystalline Ti-6242 specimen at a low magnification (200×) under the operating conditions (i.e. accelerating voltage, spot size, working distance and stage tilt) that were subsequently used for the EBSD data collection on the fracture facets. The background subtraction improved the quality of the EBSD patterns obtained from the fracture facets. The operating conditions for EBSD experiments were as follows: accelerating voltage = 20 kV, working distance = 21 mm and SEM stage tilt = 70°. Increasing the number of frames to be averaged for the facet characterization also helped improve the quality of EBSD patterns. The bands in the EBSD patterns so obtained were detected manually and the patterns indexed using the computer software (supplier: TSL, Draper, UT) to determine crystallographic orientation for several locations on a particular dwell-fatigue fracture facet. In order to appropriately indicate the crystallographic orientation of the facet using an inverse pole figure, the determination of the spatial orientation of the fracture facet was necessary, which will be described next.

The spatial orientation of the dwell-fatigue fracture facets was determined using a quantitative tilt fractography technique in the SEM. This technique involves obtaining SEM images of the facets at two different tilt angles. The coordinates of three non-collinear fracture features on any one facet are measured on the SEM images at the two tilt angles. Thereafter, the coordinates of any fracture feature

'A', in the SEM stage axes system, are calculated using the relations (see Ref. [6] for derivation):

$$X^{A} = (x_1^{A} \cdot \sin\theta_2 - x_2^{A} \cdot \sin\theta_1)/\sin(\theta_2 - \theta_1) \quad (1a)$$

$$Y^{A} = y_1^{A} = y_2^{A} = (y_1^{A} + y_2^{A})/2 \quad (1b)$$

$$Z^{A} = (-x_1^{A}.\cos\theta_2 + x_2^{A}.\cos\theta_1)/\sin(\theta_2 - \theta_1) \quad (1c)$$

where (x_1^{A}, y_1^{A}) and (x_2^{A}, y_2^{A}) are the coordinates of a particular feature 'A' at tilt angles θ_1 and θ_2, respectively. X^{A}, Y^{A}, and Z^{A} denote the coordinates of point 'A' in the SEM stage axes system (***X***, ***Y***, and ***Z***). ***X***-direction of the SEM stage axes system points to the top of the SEM images, ***Y***-direction to the left of the SEM images and ***Z***-direction is anti-parallel to the electron beam direction. The fractured specimens had been placed in the SEM specimen chamber such that their longitudinal direction (i.e. the loading axis during the dwell-fatigue testing) is aligned with the ***Z***-direction of the SEM stage axes system.

Equation (1a–c) are used to calculate the coordinates (X^{B}, Y^{B}, Z^{B}) and (X^{C}, Y^{C}, Z^{C}) in the SEM stage axes system of two additional fracture features 'B' and 'C', respectively. The vector connecting point 'A' to point 'B' is given by:

$$\overrightarrow{AB} = (X^{B} - X^{A})\,\mathbf{i} + (Y^{B} - Y^{A})\,\mathbf{j} + (Z^{B} - Z^{A})\,\mathbf{k} \quad (2)$$

where **i**, **j** and **k** are the unit vectors along ***X***, ***Y*** and ***Z*** (SEM stage axes system), respectively. Similarly, the vector connecting point 'B' to point 'C' is given by:

$$\overrightarrow{BC} = (X^{C} - X^{B})\mathbf{i} + (Y^{C} - Y^{B})\mathbf{j} + (Z^{C} - Z^{B})\mathbf{k} \quad (3)$$

The cross product of these two vectors, $\overrightarrow{AB}$ and $\overrightarrow{BC}$, gives the vector representing the facet plane normal ($\vec{n}$):

$$\vec{n} = \begin{vmatrix} \mathbf{i} & \mathbf{j} & \mathbf{k} \\ (X^{B} - X^{A}) & (Y^{B} - Y^{A}) & (Z^{B} - Z^{A}) \\ (X^{C} - X^{B}) & (Y^{C} - Y^{B}) & (Z^{C} - Z^{B}) \end{vmatrix} \quad (4a)$$

i.e.

$$\begin{aligned} \vec{n} = \{&(Y^{B} - Y^{A}).(Z^{C} - Z^{B}) - (Z^{B} - Z^{A}).\\ &(Y^{C} - Y^{B})\}\mathbf{i} - \{(X^{B} - X^{A}).(Z^{C} - Z^{B}) -\\ &(Z^{B} - Z^{A}).(X^{C} - X^{B})\}\,\mathbf{j} + \{(X^{B} - X^{A}).\\ &(Y^{C} - Y^{B}) - (Y^{B} - Y^{A}).(X^{C} - X^{B})\}\mathbf{k} \end{aligned} \quad (4b)$$

A similar approach for the calculation of facet plane normal has been used by Slavik et al. [9]. The angle between the loading axis (***Z***) and the facet plane normal ($\vec{n}$) is calculated using the formula:

$$\alpha = \cos^{-1}\left(\frac{\vec{n}.\mathbf{k}}{|\vec{n}|}\right) \quad (5)$$

This quantitative tilt fractography technique was first applied on a polished smooth specimen under the operating conditions used for imaging of the fracture surfaces. The analysis gave the angle between the ***Z***-axis and the normal to the plane of polish as less than 1° and therefore, this technique is believed to be very reliable. Thereafter, this technique was applied on the dwell-fatigue fracture facets and the results are discussed in the next Section.

The quantitative tilt fractography and the EBSD experiments were completed on a particular facet in one SEM session. Care was taken not to rotate the SEM stage in order to keep the orientation of the fracture facet the same for the two sets of experiments (quantitative tilt fractography and EBSD). Based on the EBSD analysis results, the inverse pole figure was plotted for the direction that represents the fracture facet normal (Eq. 4). This inverse pole figure describes the crystallographic orientation of the dwell-fatigue fracture facet being characterized. The inverse pole figures for fracture facets are presented below.

Results and discussion

In order to obtain an idea about the orientation of the large faceted area with respect to the loading axis, the quantitative tilt fractography experiments were conducted on the faceted region shown in Fig. 2. As described in the last section, the SEM fractographs of the same area were obtained at two tilt angles, 0° and 50° (Fig. 2). A recognizable feature on the fractographs was chosen as origin, labeled as 'X' in Fig. 2a, b. It should be noted that the fracture features labeled 'X' in Fig. 2a, b are one and the same. Three additional recognizable features on the fractographs were identified and are labeled 'A', 'B' and 'C' in Fig. 2a, b. Similar to the case of the feature labeled 'X', the features labeled 'A', 'B' and 'C' in Fig. 2a correspond to 'A', 'B' and 'C', respectively in Fig. 2b. The *x* and *y* coordinates of the points 'A', 'B' and 'C', with respect to the origin 'X', were measured at both the tilt angles, 0° and 50° (Fig. 2a, b). Since tilt axis is along the ***Y***-direction, the *x* coordinates of the points 'A', 'B' and 'C' change with a change in the tilt angle whereas the *y* coordinates remain essentially unchanged. From the (*x*, *y*) coordinates of the points 'A', 'B' and 'C' at the two tilt angles, their *X*, *Y* and *Z* coordinates were determined (using the relations (1)) in

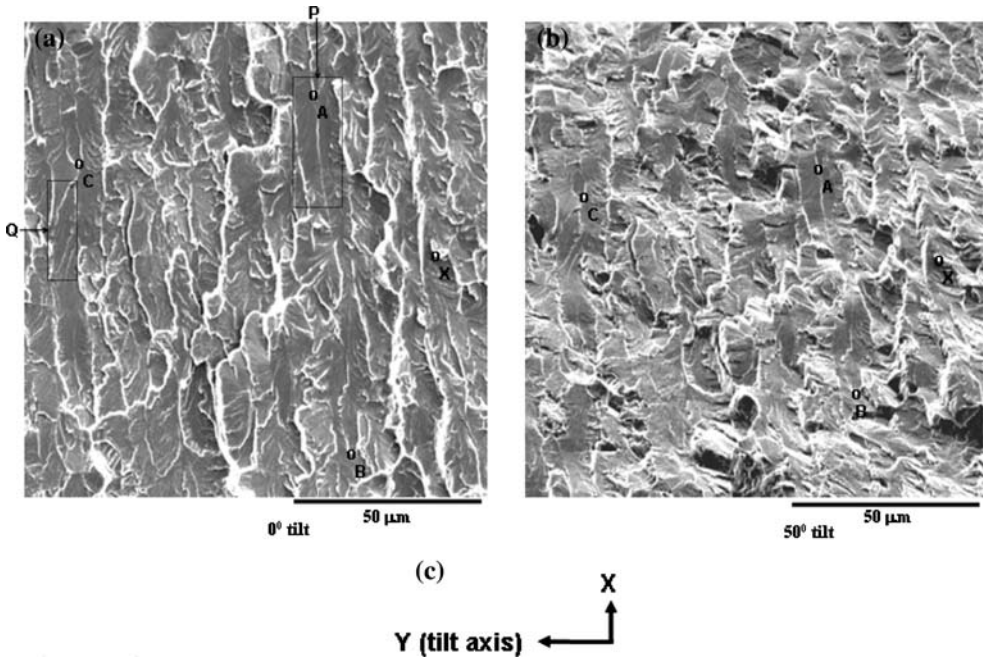

Fig. 2 SEM images of the faceted region at two different tilt angles. (**a**) 0° tilt, and (**b**) 50° tilt. Four recognizable features are labeled 'X', 'A', 'B' and 'C' in the SEM images. The points labeled 'X', 'A', 'B' and 'C' refer to the same features in (**a**) as in (**b**). The facets complementary to 'P' and 'Q' in (**a**), on the other fracture surface of the same specimen are shown at a higher magnification in Figs. 4**a** and 5**a**, respectively. (**c**) Schematic representation of the orientation of SEM stage axes system with respect to the SEM images. ***X***-axis points to the top of SEM image, ***Y***-axis to the left and ***Z***-axis is coming out of the plane of paper. The origin of the SEM stage axes system is effectively at point labeled 'X' in SEM images, for the purposes of quantitative tilt fractography analyses. The orientation of the SEM stage axes system with respect to the SEM images remains same in Figs. 3–5

the SEM stage axes system with the origin at point labeled 'X' in Fig. 2a, b. Thereafter, the vectors connecting point 'A' to 'B', and point 'B' to 'C' at 0° tilt are calculated using relations (2) and (3). The vector representing the facet (defined by points 'A', 'B' and 'C') normal, at 0° tilt, is **i**–2.4 **j** + 35.19 **k**, as calculated using relation (4). The angle between the loading axis and the facet plane normal is ~4°, as determined using Eq. 5. From this result one might conclude that the dwell-fatigue fracture facets are approximately normal to the loading axis. However, it should be noted that the analysis presented above is for a region that contains several facets. More specifically, all the facets between points 'A' and 'B', and points 'B' and 'C' (Fig. 2) are included in the calculations. If we were to focus our attention on one particular facet, we might obtain somewhat different result, as will be discussed next.

The quantitative tilt fractography analyses were done on individual facets as per the procedures described above. The only difference was that the SEM images were acquired at a much higher magnification than in Fig. 2. An example of the analyses conducted separately on the two adjacent dwell-fatigue facets is presented in Fig. 3. As before, an origin 'X' was selected at both the tilt angles. Moreover, three additional points ('A', 'B' and 'C') on facet I and three points ('D', 'E' and 'F') on facet II were identified. From the measurements of the coordinates of these six points at the two tilt angles, the vector representing the facet normal was determined for both the facets. The angle between the loading axis and facet normal is 18° for facet I and 15° for facet II. Therefore, the individual facets are oriented at 72°–75° to the loading axis even though the region encompassing several facets is approximately normal to the loading axis.

The quantitative tilt fractography analysis was conducted on one additional dwell-fatigue fracture facet (shown later in Fig. 5a) and the results are summarized in Table 1. From Table 1 it is clear that the individual facet normal is oriented at 12°–18° with respect to the loading axis.

The crystallographic orientation of the facets I and II in Fig. 4a are shown in the inverse pole figures (Fig. 4b, c). The EBSD analyses were done at five locations on facet I and three locations on facet II, as indicated in Fig. 4a. It should be mentioned that a small image drift (~1 μm) in the + ***X***-direction (the orientation of ***X***-axis with respect to the SEM images is shown in Fig. 2c) was noticed during the time needed (~10 min) for manual detection of the bands and computer software-aided indexing of multiple EBSD patterns. Nonetheless, it was ensured that all the points for which the EBSD analyses were conducted cor-

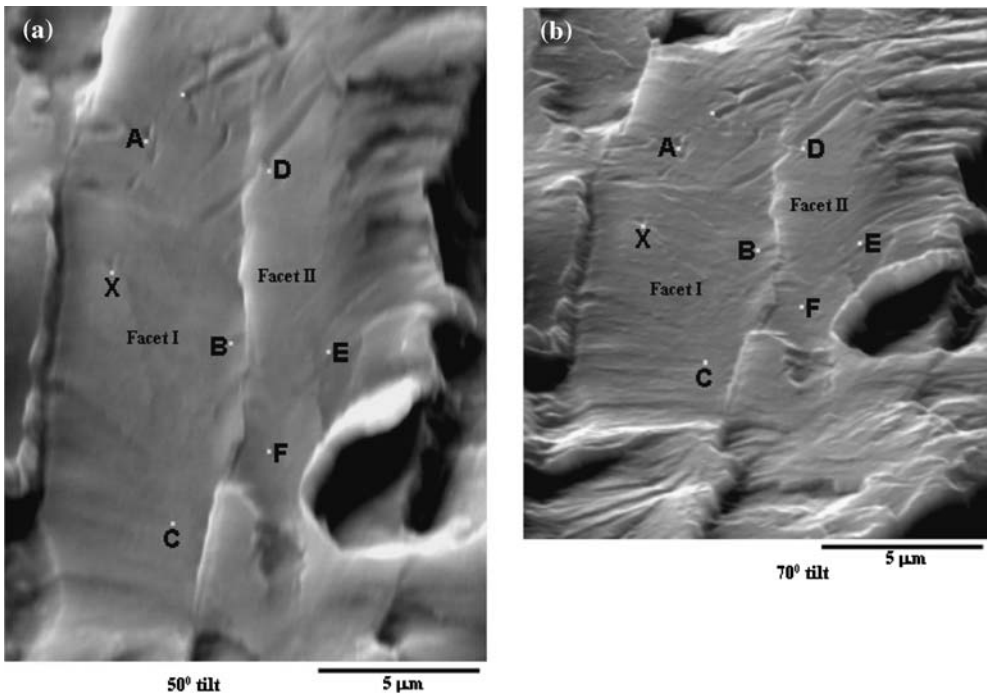

Fig. 3 SEM images of the dwell-fatigue fracture facets at two different tilt angles. (**a**) 50° tilt, and (**b**) 70° tilt. Seven recognizable features are labeled 'X', 'A', 'B', 'C', 'D', 'E' and 'F' in the SEM images. The point labeled 'X' refers to the same feature in (**a**) as in (**b**). Similarly, the points labeled 'A', 'B', 'C', 'D', 'E' and 'F' refer to the same features in (**a**) and (**b**)

responded to the facet under consideration. The inverse pole figures (Fig. 4b, c), based on the EBSD analyses at multiple locations on facets I and II, indicate a good reproducibility of the overall methodology used to determine the crystallographic orientation of individual facets. It is also clear from Fig. 4b, c that the dwell-fatigue fracture facets are not exactly aligned with the basal plane, but are inclined at ~10° to it. It is important to note that if one were to assume that the fracture facets are approximately normal to the loading axis based on the analysis presented in Fig. 2 and were to plot an inverse pole figure for the case of facet normal being aligned with the loading axis, it would result in an inaccurate representation of the crystallographic orientation of the facet. Figure 4d is such an inverse pole figure for facet I of Fig. 4a, where the facet normal has been assumed to be along the loading axis. A comparison of Fig. 4b, d indicates the degree of error that can be caused by such an assumption. Therefore, it is important to apply the quantitative tilt fractography technique to determine the orientation of the individual facets, as we have described above. Another dwell-fatigue fracture facet is shown in Fig. 5a and its crystallographic orientation is depicted in Fig. 5b. Similar to the facets I and II in Fig. 4a, the facet shown in Fig. 5a is inclined at ~10° to the basal plane.

Therefore, the dwell-fatigue fracture facets are not exactly aligned with the basal plane, but are inclined at ~10° to it. Davidson and Eylon [1] have reported similar orientation of facets, near the fracture origin, for IMI 685 dwell specimens. Blackburn and Williams [12] have also determined the crystallographic orientation of facets in Ti-8Al alloy using back-reflection X-ray techniques and our results on dwell-fatigue fracture facets are consistent with their results.

For the three dwell-fatigue facets characterized in the current study, the orientations of the facet normal and the loading axis are shown in Fig. 6a, b, respectively. The inclination of facet normal with respect to the basal plane normal lies in the range of 8°–12° with an average of ~10° (Fig. 6a). On the other hand, the inclination of loading axis with respect to the basal plane normal lies in the range of 14°–20° with an average of ~17° (Fig. 6b).

An example of the EBSD pattern obtained from a dwell-fatigue fracture facet in the current study is shown in

Table 1 Summary of quantitative tilt fractography results

Reference figure	Vector representing the facet normal ($\vec{n}$)	Angle between facet normal ($\vec{n}$) and loading axis
Fig. 2	**i**–2.40 **j** + 35.19 **k**	4°
Figs. 3 and 4 (facet I)	–**i** + 6.63 **j** + 20.02 **k**	18°
Figs. 3 and 4 (facet II)	–**i** + 6.12 **j** + 23.62 **k**	15°
Fig. 5a	–**i** +2.60 **j** +12.89 **k**	12°

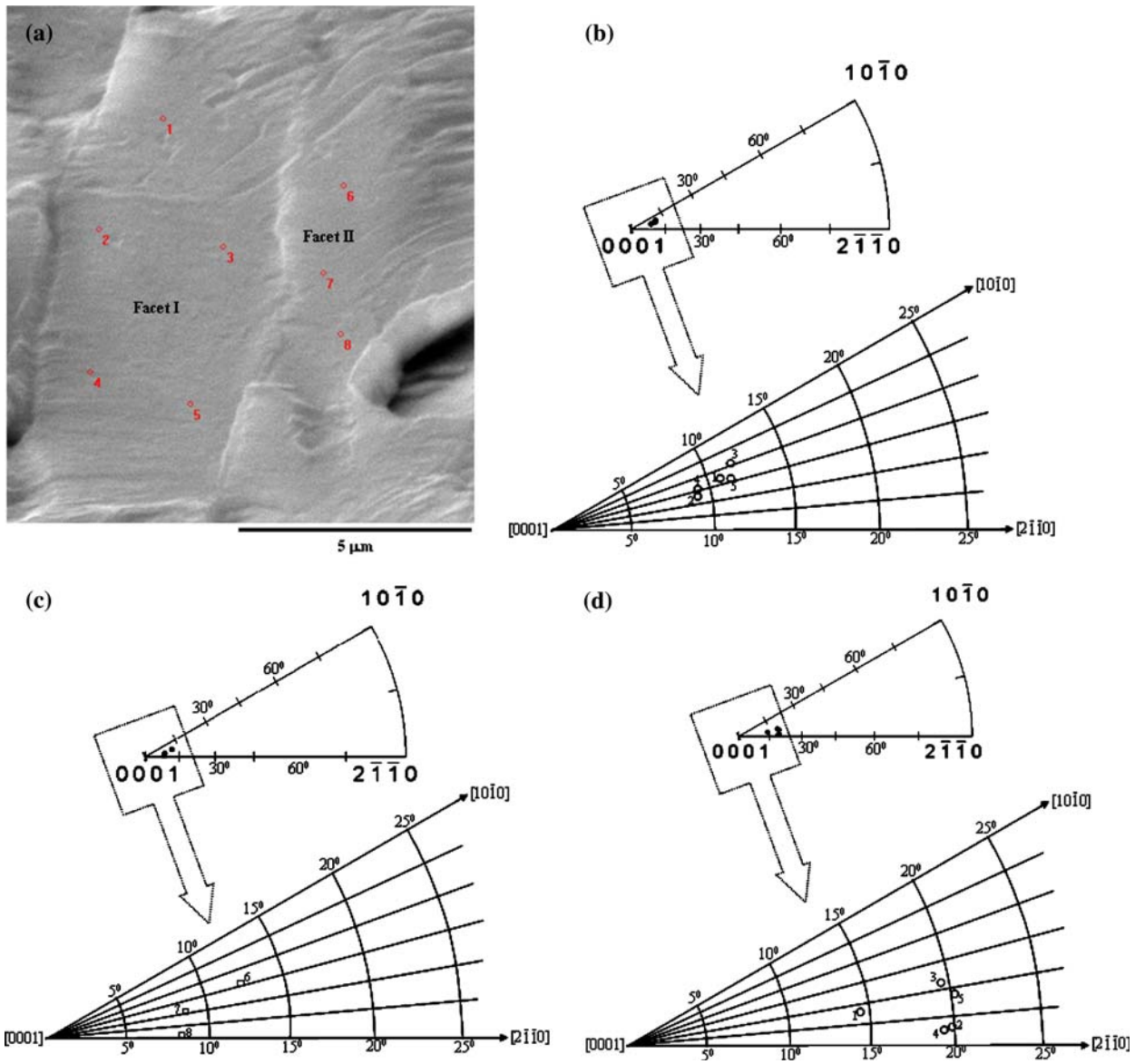

Fig. 4 Crystallographic orientation determination of individual dwell-fatigue fracture facets. (**a**) SEM image at 70° tilt of two adjacent facets I and II showing the locations of five points on facet I and three points on facet II from where the EBSD patterns were obtained and subsequently indexed to determine the crystallographic orientation of the grains across which these two facets had been produced. (**b**) Inverse pole figure showing the position of facet I normal based on the EBSD analyses on five locations shown in (**a**) and the spatial orientation of the facet (facet normal, $\vec{n} = -\mathbf{i} + 6.63\,\mathbf{j} + 20.02\,\mathbf{k}$), as determined by the quantitative tilt fractography technique (see Fig. 3 and Table 1). (**c**) Inverse pole figure showing the position of facet II normal based on the EBSD analyses on three locations shown in (**a**) and the spatial orientation of the facet (facet normal, $\vec{n} = -\mathbf{i} + 6.12\,\mathbf{j} + 23.62\,\mathbf{k}$), as determined by the quantitative tilt fractography technique (see Fig. 3 and Table 1). (**d**) Inverse pole figure showing the position of facet I normal based on the EBSD analyses on five locations shown in (**a**) and assuming the facet to be normal to the loading axis, i.e. $\vec{n} \parallel \mathbf{k}$ (Please see text for details)

Fig. 7a. Part of the phosphor screen in our laboratory is damaged and this keeps part of the pattern (labeled 'A' in Fig. 7a) from being detected. Furthermore, there is another dark region (labeled 'B' in Fig. 7a) which is caused due to the fact that the facet plane is not perpendicular to the electron beam at 0° tilt (as is the case for the specimens polished specifically for EBSD analysis). The result of the indexing of the pattern shown in Fig. 7a, using the technique outlined in the current paper, is shown in Fig. 7b. It is clear that in spite of part of the EBSD pattern missing, the indexing yields an unambiguous (Fig. 7b) and reproducible (see Figs. 4 and 5) crystallographic orientation.

It is important to note that the typical spot size for the electron channeling technique is ~50 μm [1], whereas it is much less than 1 μm for the EBSD-based technique described in the present paper. Therefore, significantly smaller facets can be characterized using the latter technique. Furthermore, the facets were electropolished for

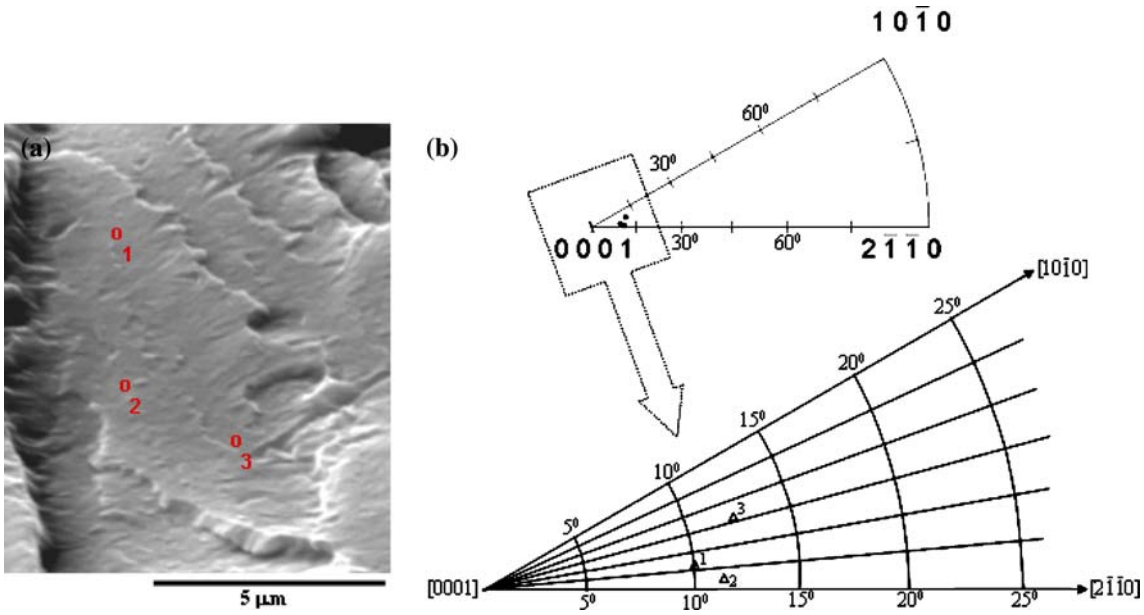

Fig. 5 Crystallographic orientation determination of another dwell-fatigue fracture facet. (**a**) SEM image at 70° tilt of a facet showing the locations of three points on the facet from where the EBSD patterns were obtained and subsequently indexed to determine the crystallographic orientation of the grain across which this facet had been produced. (**b**) Inverse pole figure showing the position of the facet normal based on the EBSD analyses on three locations shown in (**a**) and the spatial orientation of the facet (facet normal, $\vec{n} = -\mathbf{i} + 2.60\,\mathbf{j} + 12.89\,\mathbf{k}$), as determined by the quantitative tilt fractography technique (see Table 1)

characterization by electron channeling technique in the work of Davidson and Eylon [1]. In the current study, the EBSD patterns were obtained directly from the fracture facet and the electropolishing of facets was not needed. Thus, the alloys with finer microstructural features are amenable to the characterization by the technique presented in the current paper, because electropolishing causes a loss of finite thickness of material. Moreover, the technique proposed in the current paper is simpler to apply because it does not require electropolishing of the fracture facets.

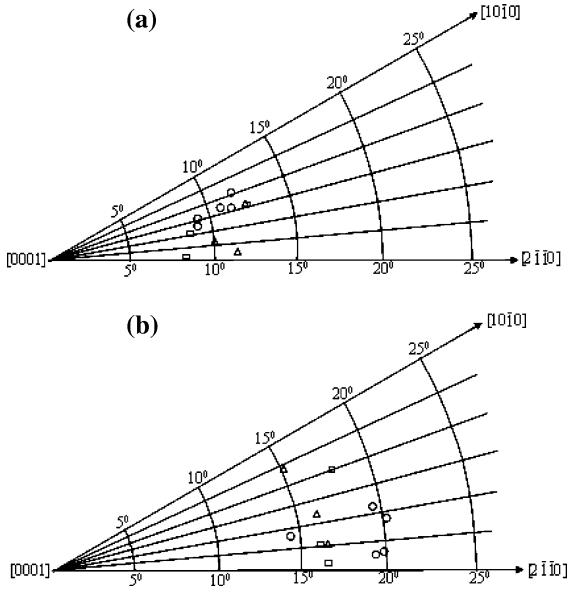

Fig. 6 Inverse pole figures showing the orientation of (**a**) facet normal, and (**b**) loading axis for the facets shown in Figs. 4**a** and 5**a**. ○: Facet I of Fig. 4**a**; □: Facet II of Fig. 4**a**; and Δ: Facet shown in Fig. 5**a**

The technique of the current work has been used to determine the crystallographic orientation of fracture facets in Ti-6242 that are produced under three different loading conditions (normal - fatigue, dwell - fatigue and static - loading) and those results are reported elsewhere [10].

Summary and conclusions

In this paper, a technique to determine the crystallographic orientation of the fracture facets has been described. The spatial orientation of the facet plane was determined by the quantitative tilt fractography technique in an SEM. The crystallographic orientation of the grain, across which the fracture facet had been produced, was determined by EBSD analysis, also in an SEM. These two pieces of information were combined to obtain the crystallographic orientation of the fracture facets.

In the technique proposed in this paper, electropolishing of the fracture facets is not needed and the EBSD patterns are obtained directly from the facets. Thus, this technique is simpler and more straightforward than the electron

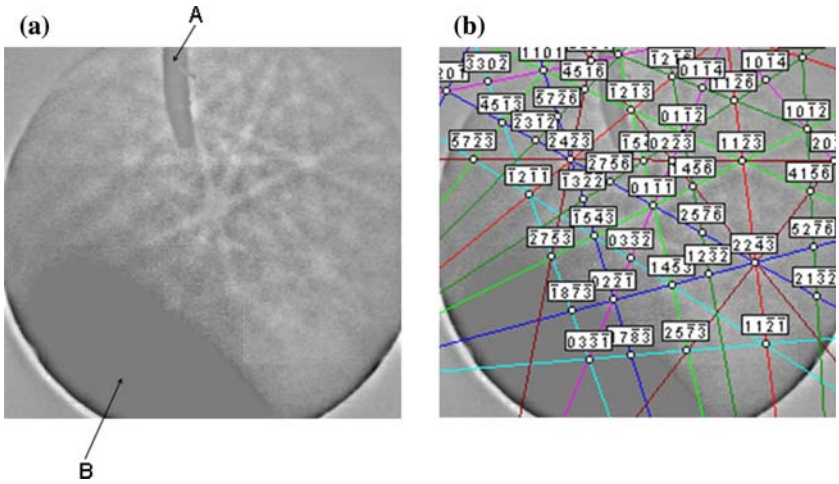

Fig. 7 (**a**) An example of the EBSD pattern obtained from the facet I shown in Fig. 4a, and (**b**) indexing of the pattern shown in (**a**). Parts of the pattern are not detected: the region labeled 'A' in (**a**) is due to the damage in this small part of the phosphor screen, whereas the region labeled 'B' is due to the fact that the fracture facet is not exactly normal to the electron beam prior to tilting for the EBSD and the quantitative tile fractography experiments. Even with part of the pattern missing, the indexing yields an unambiguous, correct and reproducible result

channeling technique employed by Davidson and Eylon [1]. The spot size for the EBSD analysis is much less than 1 μm, whereas it is typically ~50 μm for the electron channeling technique [1]. Therefore, an alloy with finer microstructural features and smaller fracture facets can be characterized using the technique described in the current paper.

Though Bache et al. [3] have obtained the EBSD patterns directly from the fracture facets in a Ti-alloy after a light etch, the determination of the spatial orientation of the fracture facets has not been discussed explicitly in their work. Davies et al. [13] have also conducted EBSD analysis directly on the cleavage facets in steel. As has been discussed in the current paper and in prior studies [7–9], the determination of the spatial orientation of the fracture facets is essential for an appropriate determination of their crystallographic orientation, unless the specimen is oriented to make the facet plane perpendicular to the electron beam (as Davidson and Eylon [1] have done in their work) prior to tilting for the EBSD experiments. We have described a technique to determine the spatial orientation of the fracture facets, which is based on the work of Themelis et al. [6].

We have used the technique described in the current paper to determine the crystallographic orientation of several dwell-fatigue fracture facets in Ti-6242 alloy. Our results indicate that these facets are inclined at ~10° to the basal plane.

In another work [10], we have used the technique described in the current work to characterize the fracture facets at the crack-initiation site in the same Ti-6242 alloy for different loading conditions.

Acknowledgments This research was supported by the Federal Aviation Administration. The authors thank the Technical Monitor, Joseph Wilson, for his encouragement and support of this work. The donation of Ti-6242 pancake forging by Ladish Co. Foundation (Cudahy, WI) is also gratefully acknowledged.

References

1. Davidson DL, Eylon D (1980) Metallurgical Transactions 11A:837
2. Bache MR, Davies HM, Evans WJ (1995) Titanium '95: Science and Technology, p 1347
3. Bache MR, Evans WJ, Davies HM (1997) Journal of Materials Science 32:3435
4. Woodfield AP, Gorman MD, Corderman RR, Sutliff JA, Yamrom B (1995) Titanium '95: Science and Technology, p 1116
5. Sinha V, Mills MJ, Williams JC (2004) Metallurgical and Materials Transactions 35A:3141
6. Themelis G, Chikwembani S, Weertman J (1990) Materials Characterization 24:27
7. Semprimoschnig COA, Stampfl J, Pippan R, Kolednik O (1997) Fatigue & Fracture of Engineering Materials & Structures 20(11):1541
8. Davies PA, Randle V (2001) Journal of Microscopy 204(Pt 1):29
9. Slavik DC, Wert JA, Gangloff RP (1993) Journal of Materials Research 8(10):2482
10. Sinha V, Mills MJ, Williams JC (2006) Metallurgical and Materials Transactions 37A: 2015–2026
11. Wright SI (2000) In: Schwartz AJ, Kumar M, Adams BL (eds) Electron backscatter diffraction in materials science. Kluwer Academic/Plenum Publishers, New York, NY, p 51
12. Blackburn MJ, Williams JC (1969) Metallurgical aspects of the stress corrosion cracking of Titanium alloys,'' Proc. Conf. on the Fundamental Aspects of Stress Corrosion Cracking, N.A.C.E., p 620
13. Davies PA, Novovic M, Randle V, Bowen P (2002) Journal of Microscopy 205(Pt 3):278